A novel mid-infrared hollow waveguide gas sensor for measuring water vapor isotope ratios in the atmosphere

Yang Liu[a], Tao Wu[a*], Qiang Wu[b], Weidong Chen[c], Chenwen Ye[a], Mengyu Wang[a], Xingdao He[a]

[a]Jiangxi Provincial Key Laboratory of Opto-Electronic Information Science and Technology, Nanchang Hangkong University, Nanchang, 330063, China

[b]Department of Mathematics, Physics and Electrical Engineering, Northumbria University, Newcastle upon Tyne, NE1 8ST, UK

[c]Laboratoire de Physicochimie de l'Atmosphère,Université du Littoral Côte d'Opale 189A, Av. Maurice Schumann, Dunkerque 59140, France

*E-mail: wutccnu@nchu.edu.cn

Abstract:

A novel mid-infrared hollow waveguide gas sensor was developed to target $H_2{}^{18}O$, $H_2{}^{16}O$, $H_2{}^{17}O$, and HDO absorption lines at 3662.9196, 3663.04522, 3663.32128, and 3663.84202 cm^{-1}, respectively, based on wavelength modulation spectroscopy using a 2.73μm distributed feedback diode laser. A hollow waveguide fiber with a 5-m length and 1-mm inner diameter was used for gas absorption. A dew point generator with liquid water with known water–isotope ratios was used to calibrate the sensor. Detection limits of 35.18 ppbv, 4.69 ppmv, 60.53 ppbv, and 3.88 ppbv were obtained for $H_2{}^{18}O$, $H_2{}^{16}O$, $H_2{}^{17}O$, and HDO, respectively, in a 96-s integration time, which resulted in isotopic ratio measurement precision of 0.85‰, 0.57‰, and 10.48‰ for $\delta^{18}O$, $\delta^{17}O$, and δD, respectively. Field measurements of $H_2{}^{18}O$, $H_2{}^{16}O$, and $H_2{}^{17}O$ concentration were conducted on the Nanchang Hangkong University campus to evaluate sensor performance.

Keywords: Hollow waveguide, Gas sensor, Wavelength modulation spectroscopy, Water vapor–isotope ratio

1 Introduction

Water isotopes ($H_2{}^{16}O$, $H_2{}^{18}O$, $H_2{}^{17}O$, HDO) exist in various mass and combination forms. Phase transformation results in further fractionation of water isotopes. Light water isotopes are preferentially evaporated, whereas heavy isotopes are preferentially condensed. These phenomena considerably affect atmospheric physical characteristics, such as water migration and water vapor exchange and transmission, in water phase transformation, which is widely used as a climate information index in paleoclimate reconstruction and current water cycle research. In particular, the isotopic ratio in polar ice cores is used to reconstruct past temperature [1,2]. The isotopic ratio of high-altitude ice cores and stalagmites in middle and low latitudes has been used to reconstruct the paleoclimate and precipitation rate [3-5]. Water vapor isotopologues in the upper troposphere and lower stratosphere can act as ideal tracers to test the various mechanisms of stratospheric aridity. Stable isotopes of water exhibit unique advantages in the atmospheric water cycle and atmospheric circulation simulation [6,7].

Isotope ratio mass spectrometry (IRMS) and isotope ratio laser spectrometry (IRLS) are typically used for isotopic ratio measurement. IRMS is a conventional method used for isotope ratio analysis [8]. Although the method can satisfy research requirements, it exhibits inherent disadvantages. IRMS instruments are bulky, expensive, and require well-trained technicians for operation, especially for the measurement of water isotopic ratio. Because of the condensation of water samples, the mass spectrometer cannot be directly used for analysis. Water samples should be first chemically transformed into gases, such as H_2 and CO_2, which can be easily analyzed, to determine the isotopic ratio of ^2H and ^{18}O [9]. However, H_2 is usually produced by reduction of water over hot (~800 °C) uranium [10] or zinc [11] to determine δ^2H. These chemical pretreatments are dangerous and time consuming, which limits its application and renders changing the measurement site at any time for real-time online measurement difficult. Because the molecular mass of $^{17}O^{12}C^{16}O$ and $^{16}O^{13}C^{16}O$ are the same, the isotopic ratio of ^{17}O cannot be measured.

IRLS technology is an alternative isotope measurement technology that exhibits a measurement accuracy that is comparable to the IRMS method. Furthermore, time consuming and chemical pretreatment are not required. Small volume and fast

response time are critical for the miniaturization of instruments and online real-time detection. The IRLS method for measuring hydrogen and oxygen isotopes of water vapor has been widely applied to studies climate change, ecological cycle, and biomedicine. Kerstel et al. measured the abundance ratio of hydrogen and oxygen isotopes in low-pressure gas-phase water by means of tunable diode laser spectroscopy (TDLAS) at 1.39 μm [12] and 2.7 μm [13]. Kerstel et al. [14-15] reported a compact, high-finesse optical-feedback CEAS spectrometer (OF-CEAS) for measuring water vapor isotope with a low concentration at 1.39 μm. Castrillo et al. [16] measured the isotope ratio $^{17}O/^{16}O$ in water by offset-frequency locked extended-cavity diode lasers at 1.39 μm with a precision of 0.6 ‰. Gianfrani et al. [17] measured the $^{2}H/^{1}H$, $^{17}O/^{16}O$, and $^{18}O/^{16}O$ isotope ratios in water by TDLAS using a pair of 1.4-μm diode lasers. Dyroff et al. [18] developed a TDLAS instrument for airborne measurements of $^{18}O/^{16}O$ and D/H isotope ratios of water at 2.66 μm. Wu et al. [19, 20] measured the isotope ratios D/H, $^{18}O/^{16}O$, and $^{17}O/^{16}O$ in water through TDLAS with a 20 m multi-pass cell (MPC) at 2.73 μm. Cui et al. [21] analyzed the $^{18}O/^{16}O$, $^{17}O/^{16}O$, and D/H isotope ratios in glacier water by TDLAS at 2.73 μm with a 100 m MPC . McManus et al. [22] designed a dual-laser instrument for measuring isotopologues of carbon dioxide at 4.3 μm and water at 2.77 μm. Lee et al. [23-24] measured D/H and $^{18}O/^{16}O$ in atmospheric water vapor based on TDLAS at 6.66 μm. Sayres et al. [25] used off-axis cavity-enhanced absorption spectroscopy (OA-ICOS) to measure the abundances of two isotopic molecules, HDO and $H_2{}^{18}O$, in water vapor in the stratosphere. Wang et al. [26] designed a mid-infrared quantum cascade laser spectrometer to measure $H_2{}^{16}O$ and $H_2{}^{18}O$ at 7.12 μm. Table 1 summarized water isotope ratio measurements by various laser spectrometry methods reported in the literature and the corresponding key experimental parameters. Picarro Inc. [27] and LGR Inc. [28] develop water vapor isotope analyzers by using cavity ring-down and cavity enhanced spectroscopy technology, which enables simultaneous measurement of $\delta^{2}H$, $\delta^{18}O$, and $\delta^{17}O$ of water vapor with high precision (0.05‰ for $\delta^{18}O$, 0.05‰ for $\delta^{17}O$, and 0.2‰ for $\delta^{2}H$).

Table 1 Summary of water isotope ratio measurements by various laser spectrometry methods reported in the literature and the corresponding key experimental parameters.

Ref.	λ (μm)	Method	Cell	L_{eff} (m)	Volume (mL)	C (ppm)	Precision (‰)		
							$\delta^{2}H$	$\delta^{17}O$	$\delta^{18}O$

[12]	1.39	TDLAS	MPC	20.5	-	1000000	3	1	0.5
[14]	1.39	OF-CEAS	Cavity	6150	-	200	9	3	1
[15]	1.39	OF-CEAS	Cavity	45000	-	1500	0.12	0.07	0.02
[16]	1.39	TDLAS	MPC	20	-	1000000		0.6	
[17]	1.4	TDLAS	MPC	20.5	-	1000000	0.5	0.5	0.2
[18]	2.66	TDLAS	MPC	76	500	100	4.5		1.2
[13]	2.73	TDLAS	MPC	20.5	-	1000000	0.7	0.5	0.5
[19-20]	2.73	TDLAS	MPC	20	300	1000000	0.84	0.48	0.72
[21]	2.73	TDLAS	MPC	100	300	1000000	0.64	0.13	0.13
[22]	2.77	TDLAS	MPC	36		~10000	0.3		0.1
[23-24]	6.66	TDLAS	Single cell	1.53	400	15900	1.1		0.07
[25]	6.7	OA-ICOS	Cavity	4500	-	5	50		30
[26]	7.12	TDLAS	MPC	3.5	600	15766			0.05

[a] Note that the water vapor of 1000000 ppm represents liquid water.

In conventional IRLS methods, Herriott cells and optical cavities are used as gas cells, which have a large volume (>100 mL), a large physical size, and a high cost. The hollow waveguide (HWG) fiber proposed by Garmire et al. [29] not only guides light but also samples gas. The fiber can be extended to tens of meters for high sensitivity [30] and coiled to small spaces for miniaturization. Furthermore, the anti-electromagnetic interference ability of the HWG fiber is strong, which can be used for gas detection in a harsh environment. These advantages render the HWG-fiber-based gas sensing sensors suitable for environmental monitoring, biomedical diagnosis, and industrial production.

In this study, we present the design of a mid-infrared HWG gas sensor based on a fiber absorption cell formed by a 5 m long and 1 mm inner diameter HWG fiber, combined with wavelength modulation spectroscopy (WMS) technique. $H_2{}^{18}O$, $H_2{}^{16}O$, $H_2{}^{17}O$, and HDO absorption features at 2.73μm were simultaneously targeted within the current tuning range of the laser. The Allan variance was used to evaluate the detection limit and stability of the sensor. Finally, the concentration of water vapor isotope molecules in the atmosphere was measured.

2 Experimental principle

According to the wavelength modulation spectroscopy principles [31], the amplitude of 2*f* signal for optically thin samples ($a(v)<0.05$) can be linearly expressed as follows:

$$S_{2f,L}^{in}(\bar{\nu}_a) = -\beta\eta I_0 SnL\,\bar{\chi}_{2f,L}^{even}(\bar{\nu}_a)\,, \tag{1}$$

where $\bar{\nu}_a$ ($\nu_a/\Delta\nu_L$) is the width-normalized modulation amplitude, ν_a is the modulation amplitude, $\Delta\nu_L$ is the half-width at half-maximum of the Lorentzian profile, β is the gain of the lock-in amplifier, η is the constant associated with the system, I_0 is the initial light intensity, S is the absorption line strength, n is the density of absorbers, and L is the effective absorption path length. Furthermore, $\chi_{2f,L}^{even}(\bar{\nu}_a)$ is the standardized Lorentzian lineshape function at the center of the absorption line, which is constant for the fixed modulation amplitude of the laser and constant pressure in the gas cell. Therefore, the 2*f* amplitude is linearly proportional to the gas density *n*.

The isotope ratio *R* is expressed as the ratio of the rare to the abundant isotopologues species as follows:

$$^{x}R = \frac{^{x}n}{^{a}n}, \tag{2}$$

where *x* refers to the rare isotopic species ($H_2{}^{18}O$, $H_2{}^{17}O$, and HDO), and *a* represents the abundant isotopic species ($H_2{}^{16}O$).

The deviation of the abundance ratio of the sample with respect to the international standard reference (Vienna Standard Mean Ocean Water) is expressed in terms of the δ-value as follows [32]:

$$\delta(x)‰ = \left(\frac{^{x}R_{sam}}{^{x}R_{VSMOW}} - 1\right) \times 1000 \tag{3}$$

3 Experimental section

The selection of an appropriate gas molecular absorption spectral line for isotope ratio measurement is vital and directly affects the accuracy and sensitivity of the measurements. Interference of other molecular absorption lines and measurement of two or more absorption lines within the laser wavelength tuning range are the main consideration issue. The molecular absorption lines and the ground state energy of the selected isotopes to be measured should be similar. A commercially available and compact 2.73-μm DFB laser covering the absorption lines of $H_2{}^{18}O$ (3662.9196cm^{-1}), $H_2{}^{16}O$ (3663.04522 cm^{-1}), $H_2{}^{17}O$ (3663.32128 cm^{-1}), and HDO (3663.84202 cm^{-1}) with the corresponding absorption line strengths of 2.1×10^{-23}, 8.5×10^{-23}, 7.2×10^{-23}, and 1.2×10^{-23} cm/molecule, respectively, satisfies these requirements. For the

selected pair of lines, a variation of 1 K leads to a precision of −3.1‰ for $\delta^{18}O$, −6.0‰ for $\delta^{17}O$, and −8.0‰ for $\delta^{2}H$. Figure 1 displays the spectral absorption simulation of 1.8% H_2O and 400 ppmv CO_2 at a pressure of 160 mbar in the range of 3662.77–3663.93 cm^{-1} according to the HITRAN 2016 database. Figure 1 reveals that the HDO absorption line overlaps with the CO_2 absorption line; therefore, the measurement of HDO concentration and corresponding $\delta^{2}H$ at this spectral region is available only for liquid water not for ambient water vapor.

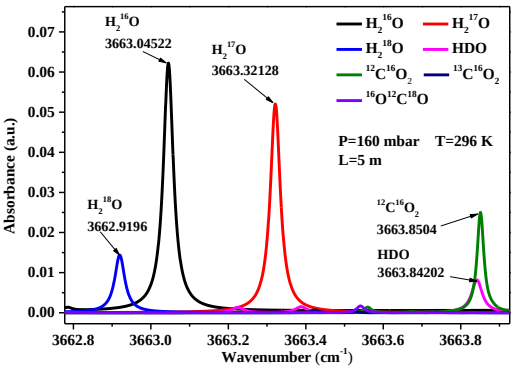

Figure 1 Simulated absorption lines of 1.8% H_2O, 400 ppmv CO_2, and its isotopes in the range of 3662.77–3663.93 cm^{-1}

Schematic of the mid-infrared HWG gas sensor is displayed in Figure 2. The figure is divided into the optical, electrical, and gas delivery parts. A DFB laser centered with the wavelength of 2.73 μm and integrated with a thermistor and a thermoelectric cooler packaged in a TO5 mount (physical size is 5×5×5 cm^3) from the Nanoplus, Gerbrunn, Germany was used as the light source for the simultaneous measurement of water vapor isotopologues ($H_2{}^{18}O$, $H_2{}^{16}O$, $H_2{}^{17}O$, and HDO). An aspheric lens was placed before the laser to collimate the emitting beam. The laser beam was injected into a 5-m-long and 1 mm-inner diameter HWG fiber (HWEA 10001600, Polymicro Technologies, USA) transparent for light from 2.6 to 10.6 μm with a max bending loss of 1.5 dB/m by a lens with a 75-mm focal length. The HWG fiber was coiled on the outer surface of a plastic hollow cylinder manufactured through 3D printing. The HWG fiber was inserted into the slot of the gas connector and sealed with silicon glue. The gas connector at the opposite end of the HWG fiber was sealed with a CaF_2 window by using an O-ring. After reflection back and forth through the inner wall of the fiber, the light was emitted from the HWG fiber and received by a photovoltaic detector (PVI-4TE-10.6, VIGO System S.A, USA). To

reduce the interference from ambient water vapor, the laser and detector were placed as close to the HWG fiber as possible.

The electrical part is used to provide laser driver signal, control the output signal of the detector, and control the temperature of the HWG fiber. The current and temperature of the laser were controlled by a commercial controller (LDC-3724, ILX Lightwave, USA) with a temperature control accuracy of 0.1°C and current output accuracy of 0.05%. A triangular signal (10 Hz and 0.3 Vpp) produced from a function generator and a sinusoidal wave (10 kHz and 0.09 V RMS) generated by a lock-in amplifier (SR830, Stanford Research System, USA) were superposed to the laser current to scan and modulate the laser wavelength. The laser modulation amplitude and modulation frequency, as well as gas pressure were all optimized. For signal processing, the output of the detector was sent to the lock-in amplifier for 2*f* demodulation at optimal sensitivity and time constants. A synchronous signal was provided by the function generator for the lock-in amplifier to ensure phase synchronization. The 2*f* harmonic signals were obtained with a 14-bit data acquisition card at a sampling rate of 40 kHz. For the selected lines of $H_2{}^{18}O$, $H_2{}^{16}O$, $H_2{}^{17}O$, and HDO in our study, the precision of the isotopic abundance measurement to 1‰ requires a temperature stability of more than 0.1 K. The HWG fiber was covered with silver foil, heater band, and insulation foam. To reduce the sticking effect of water vapor on the inner wall of the HWG fiber, the temperature of the HWG fiber was maintained at 313.15 K with an accuracy < 0.1 K using a heating belt associated with a platinum resistor and a PID controller. .

For the gas delivery system, the ambient air outside of the laboratory was sampled through a 4-meter-long PFA tube, filtered by a PTFE filter, and subsequently pumped into the HWG fiber by using a low-noise diaphragm pump (1.2 L, DIVAC, Germany). The pressure in the HWG fiber was controlled by a pressure controller (640B, MKS Instruments, USA) placed at the upstream of the HWG fiber and set to 160 mbar. The flow rate for the sampling gas was controlled by a mass flow controller (MFC, GV50A, MKS Instruments, USA) at the HWG outlet and set to 17 mL/s. The pressure difference for filling the sampling gas into the fiber was 90 mbar. A dew point generator (DPG, Li-610, Li-Cor, USA) filled with a liquid water working standard with known isotopic signatures ($\delta^{18}O$= −3.83 ‰, $\delta^{17}O$= −2.07 ‰ and $\delta^{2}H$=

−28.2 ‰) were used in the calibrations. The DPG inlet was connected to high-purity nitrogen gas. A tee-split (N_2 out in Fig. 2) was placed between the nitrogen gas and the inlet of DPG to avoid over-pressurization of the DPG. The flow rate of the DPG was set to 33 mL/s, which was faster than the sample gas flow rate. Excess water vapor flow was released into the atmosphere through another tee-split (H_2O out in Fig. 2).

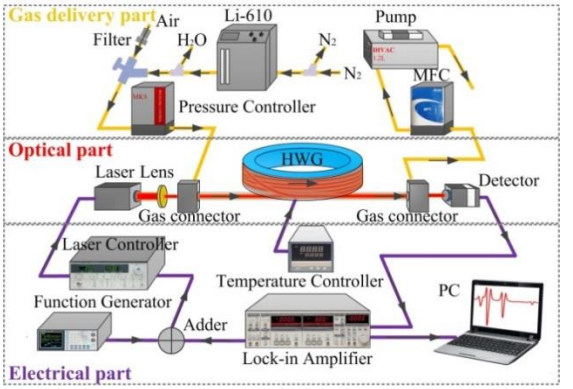

Figure 2 Schematic of the mid-infrared hollow waveguide gas sensor for simultaneous measurement of four water vapor isotopologues

5 Result and discussion

In order to obtain the calibration coefficients of 2*f* peak values and water vapor isotopologues concentrations, water vapor with various concentrations were provided by adjusting the operating temperature of the DPG. Pure nitrogen was supplied as the carrier gas for the DPG. The output gas flow contained a known water concentration determined by the set dew point temperature with an accuracy of ±0.02°C, which corresponding to water vapor concentration error of around ±20 ppm at 14°C with a relative uncertainty of 0.12 %. The dew point temperature was set from 6 to 24°C, which produced nine water vapor concentrations (0.93%, 1.06%, 1.39%, 1.58%, 1.80%, 2.05%, 2.32%, 2.62%, and 2.96%). After the set dew point temperature reached stable states, the DPG air pump was turned on. The mixture was delivered through PFA tubing by using the pressure controller into the HWG fiber. A plot of the 2*f* signals versus various water vapor concentrations is displayed in Figure 3. The etalon undulation was observed in nonabsorbance region. The free spectral range (FSR) of the etalon was 1.5 GHz, which could be resulted from light interference through two parallel surfaces of optical elements. If the reflecting surfaces were air spaced, the two parallel surfaces were separated by 10 cm. As the mid-infrared HWG

gas sensor is exposed to room air and not temperature stabilized, the etalons are unstable and changed with temperature.

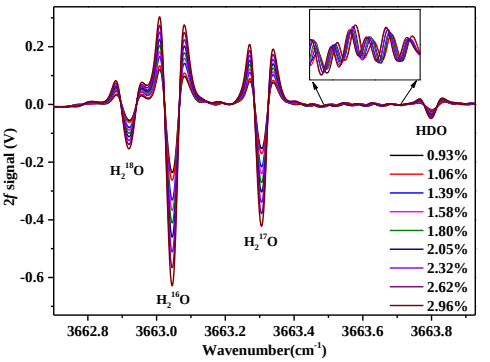

Figure 3 2*f* signals for various water vapor concentrations

According to the natural abundance of $H_2{}^{18}O$, $H_2{}^{16}O$, $H_2{}^{17}O$, and HDO, the gas concentrations of the four-water vapor isotopologues were estimated. A plot of the measured 2*f* peak values versus various four water vapor isotopologues concentrations is displayed in Figure 4. Each 2*f* peak value in Figure 4 was obtained by averaging 500 measured values for each concentration level. Figure 4 reveals that 2*f* peak values of $H_2{}^{18}O$, $H_2{}^{16}O$, $H_2{}^{17}O$, and HDO were related to their concentrations with linear correlations of 0.99915, 0.99949, 0.99985, and 0.98873, respectively. The fitted curves were used as the calibration function to determine H_2O isotopologue concentrations.

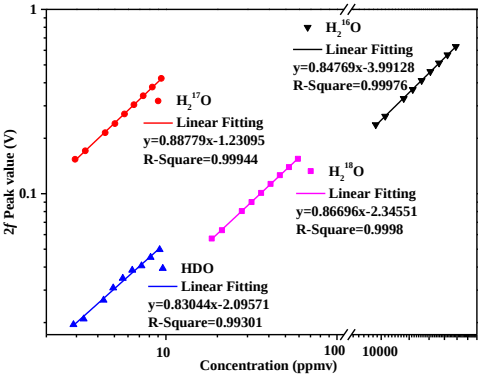

Figure 4 2*f* peak values as a function of the water vapor isotopologue concentrations

Because of the sticking of water vapor, the potential intersample memory effects on the inner wall of the HWG fiber was considered. Continuous measurement of nine widely spaced $H_2{}^{16}O$ concentration levels (1.06%, 1.21%, 1.39%, 1.58%, 1.80%, 2.05%, 2.32%, 2.62%, and 2.96%) were performed and repeated as displayed in Figure 5(a). Figure 5(a) reveals that all the measurements reached the same plateau

level. Figure 5(b) displays plots of the averaged 2*f* peak values versus various $H_2{}^{16}O$ concentration levels for two repeated measurements. The two fit curves agree well even at very high $H_2{}^{16}O$ concentration (typical ambient water mixing ratio is 1.2%). The difference in 2*f* peak values for each concentration level between two repeated measurements is displayed in Figure 5(c). The relative errors for two repeated measurements were less than 0.9%. These indicated negligible surface effects occurring on the cell and tube walls.

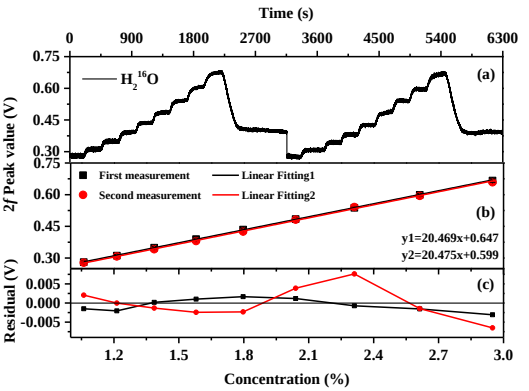

Figure 5 (a) Continuous two-time measurements of nine widely spaced $H_2{}^{16}O$ concentration levels; (b) 2*f* peak values versus various $H_2{}^{16}O$ concentrations for two repeated measurements; (c) difference in 2*f* peak values between two repeated measurements in (b)

The detection limits of water vapor isotopologues by the present mid-infrared HWG gas sensor were assessed by the Allan variance. Continuous measurements of water vapor samples were performed using a DPG-generated gas flow. The DPG was operated at the set dew point of T = 16°C to produce a water vapor concentration of 1.8%. The 2*f* signals of the four water-vapor isotopologues were measured over 10500 consecutive 0.16 s spectral scans. The 2*f* peak values measured from the 2*f* signals were converted to concentrations using the calibration curve displayed in Figure 4. Figure 6 displays the time series of the four water-vapor isotopologues' concentrations and histogram plots of the concentration distribution for the four water-vapor isotopologues. The concentration distributions of $H_2{}^{16}O$ and $H_2{}^{17}O$ were characterized by Gaussian distribution, which implied random noise dominating the 2*f* signals. Under this condition the precision improved with averaging time. Two peaks were observed in the concentration distributions of $H_2{}^{18}O$ and HDO but not for Gaussian distribution. This phenomenon was attributed to the lower $H_2{}^{18}O$ and HDO signals sensitive to the underlying time-dependent etalon signals superimposed onto the 2*f*

signals displayed in Figure 3. Then the precision improved less than expected for averaging. Allan deviation [33] plots of $H_2{}^{18}O$, $H_2{}^{16}O$, $H_2{}^{17}O$, and HDO concentrations are displayed in Fig. 6. The detection limits was 35.18 ppbv for $H_2{}^{18}O$, 4.69 ppmv for $H_2{}^{16}O$, 60.53 ppbv for $H_2{}^{17}O$, and 3.88 ppbv for HDO for a 96-s integration times. Etalon effects limited the sensitivity of the sensor.

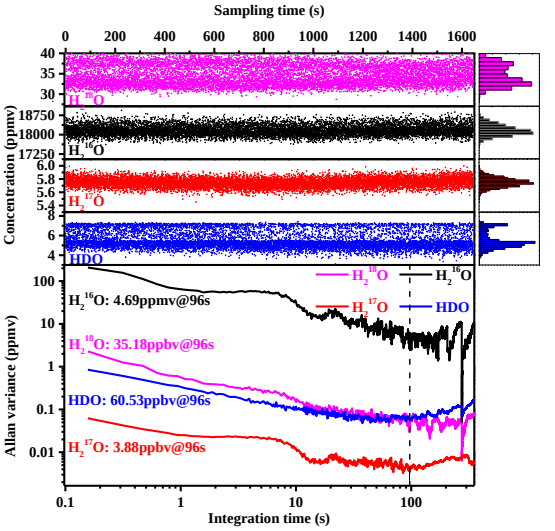

Figure 6 Time series of the measured concentrations of the four water vapor isotopologues, and the corresponding Allan deviation plots

In order to further evaluate the measurement performance of $\delta^{18}O$, $\delta^{17}O$, and δD with the present mid-infrared HWG gas sensor, $\delta^{18}O$, $\delta^{17}O$, and δD were calculated by equation (3)-(5) based on $H_2{}^{18}O$, $H_2{}^{16}O$, $H_2{}^{17}O$, and HDO concentrations data displayed in Figure 6. The Allan variance analysis was used to determine the precision of $\delta^{18}O$, $\delta^{17}O$, and δD. Figure 7 shows the time series measurements of $\delta^{18}O$, $\delta^{17}O$, and δD, as well as the corresponding Allan variances. The precisions of $\delta^{18}O$, $\delta^{17}O$, and δD are estimated as 0.85 ‰, 0.57 ‰, and 10.48 ‰, respectively, at the same optimal integration time of 96 s. The distributions and precisions of $\delta^{18}O$ and δD were affected by the etalon signals on the lower $H_2{}^{18}O$ and HDO signals, which could be reduced by balanced detection [34] or by combination of precise temperature stabilization of the entire optical sensor and background subtraction using zero-gas spectrum [26].

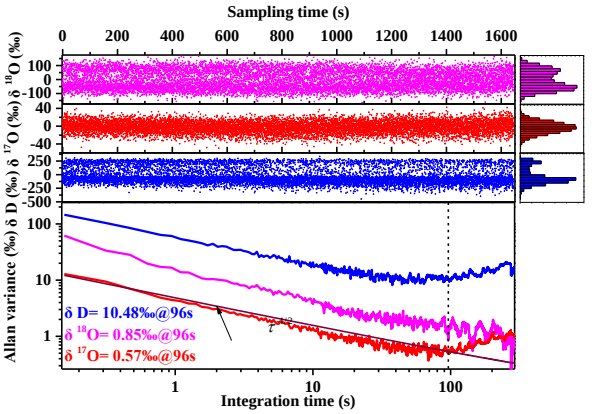

Figure 7 Time series and Allan deviation of calculated $\delta^{18}O$, $\delta^{17}O$, and δD

The performance of the mid-infrared HWG gas sensor was evaluated based on atmospheric $H_2{}^{18}O$, $H_2{}^{16}O$, and $H_2{}^{17}O$ concentration measurements on the Nanchang Hangkong University campus. Three measurements were performed using the on the daytime of July 22, 24, and 28, 2021, with continuous 6 h each day and measurement results recorded every 96 s, as displayed in Fig. 8. The $H_2{}^{18}O$, $H_2{}^{16}O$, and $H_2{}^{17}O$ concentrations were calibrated before atmospheric measurement every day. In atmospheric detection, the mid-infrared HWG gas sensor is inevitably affected by environmental noise. To improve the measurement precision of the mid-infrared HWG gas sensor, Kalman adaptive filtering was applied and analyzed. Kalman adaptive filtering as described in Refs [35, 36], the standard deviation of the first 20 measurements was used as σ_v, and the ρ value was 100. The red lines in Fig. 8 display the Kalman filtering results and the actual concentration changes. The $H_2{}^{18}O$, $H_2{}^{16}O$, and $H_2{}^{17}O$ concentrations with Kalman filtering for three daytime measurements varied from 21.85 to 30.40, 11357 to 15471, and 3.76–5.01 ppmv, with average values of 27.06, 13557.05, and 3.96 ppmv, respectively. The relatively stable concentrations of water vapor isotopologues around 50min (labeled with gray area) were selected for estimating the ambient measurement performance of water vapor isotopologues. Figure 9 shows time series of $H_2{}^{18}O$, $H_2{}^{16}O$ and $H_2{}^{17}O$ for around 50min labeled with gray area in Figure 8, and time series of the determined $\delta^{17}O$ and $\delta^{18}O$ at the same time interval. The 96 seconds measured concentrations yielded a 1 σ precision of 291.78 ppbv, 61.28 ppmv, and 15.3 ppbv for $H_2{}^{18}O$, $H_2{}^{16}O$ and $H_2{}^{17}O$, respectively. The measurement precisions of $\delta^{17}O$ and $\delta^{18}O$ were 1.78 and 11.06 ‰, respectively. The ambient measurement performance here shows slightly poorer than that

determined by the Allan variance analysis, potentially due to the instability of the system like system drift, optical fringe effect et al..

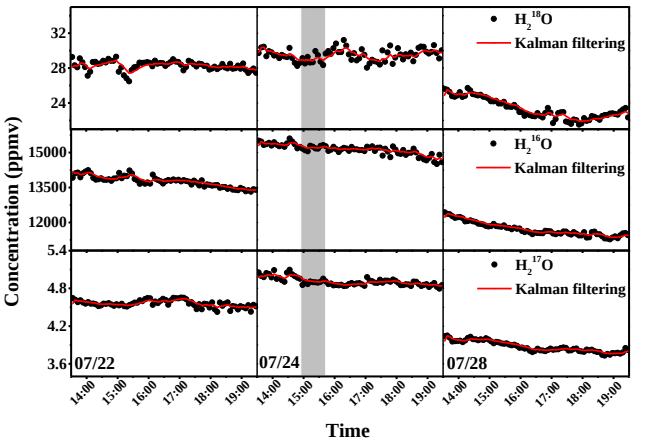

Figure 8 Time series of $H_2{}^{18}O$, $H_2{}^{16}O$, and $H_2{}^{17}O$ measured using the mid-infrared HWG gas sensor. A Kalman filter method was used to improve the detection precision (red lines).

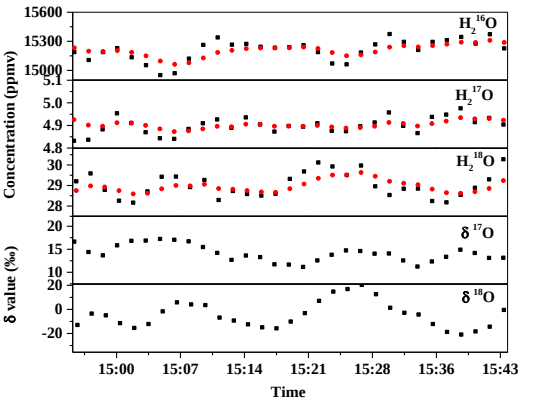

Figure 9 Time series of $H_2{}^{18}O$, $H_2{}^{16}O$ and $H_2{}^{17}O$ for around 50min labeled with gray area in Figure 8, and time series of the determined $\delta^{17}O$ and $\delta^{18}O$ at the same time interval.

Conclusion

In this study, a sensor system based on the HWG fiber was proposed to measure the isotopic abundance of water vapor by measuring concentrations of $H_2{}^{18}O$, $H_2{}^{16}O$, $H_2{}^{17}O$, and HDO as well as δ values of ^{18}O, ^{17}O, and D. Unlike conventional methods, the HWG fiber has small volume and excellent flexibility as the gas pool, which is suitable for the development of compact sensors. Standard water vapor with known concentration was produced by a dew point generator for calibration. The measured peak values of 2f signals and the water vapor isotopologue concentrations exhibited excellent linear relationships. To evaluate the measurement precision of the system,

the water vapor with a concentration of 1.8% was measured for 30 min. Allan variance analysis revealed that the detection limits of $H_2{}^{18}O$, $H_2{}^{16}O$, $H_2{}^{17}O$, and HDO were 35.18 ppbv, 4.69 ppmv, 60.53 ppbv, and 3.88 ppbv, respectively, at the integration time of 96 s. The corresponding precision of $\delta^{18}O$, $\delta^{17}O$, and δD were 0.85‰, 0.57‰, and 10.48‰, respectively. The sensor measured the water vapor isotope in the atmosphere from 13:30 to 19:30 in three days. After Kalman filtering, the variation ranges of $H_2{}^{18}O$, $H_2{}^{16}O$, and $H_2{}^{17}O$ concentrations in the atmosphere were 21.85–30.40 ppmv, 11357–15471 ppmv, and 3.76–5.01 ppmv, respectively, and the corresponding average concentrations were 27.06 ppmv, 13557.05 ppmv, and 3.96 ppmv. The 1 σ precision was 291.78 ppbv, 61.28 ppmv, and 15.3 ppbv for $H_2{}^{18}O$, $H_2{}^{16}O$ and $H_2{}^{17}O$, respectively. The measurement precisions of $\delta^{17}O$ and $\delta^{18}O$ were 1.78 and 11.06 ‰, respectively.

Acknowledgements

The authors acknowledge the support of the National Natural Science Foundation of China (Grant No. 42175130, 61965013, 61865013), the Key Research and Development Program of Jiangxi Province, China (20203BBG73039), the National Key Research and Development Program of China (No.2018YFE0115700) and Postgraduate Innovation Foundation of Nanchang Hangkong University (YC2020078).

References

[1] W. Dansgaard, The abundance of O18 in atmospheric water and water vapour, Tellus. A. 5(1953)461-469.

[2] J. Jouzel, Water stable isotopes: Atmospheric composition and applications in polar ice core studies, Trea. Geochem. 4(2003)213-243.

[3] L.G.Thompson, T. Yao, M. E. Davis, K. A. Henderson, E. Mosley-Thompson, P. Lin, Tropical climate instability: The last glacial cycle from a Qinghai-Tibetan ice core, Science. 276(1997)1821-1825.

[4] G. Hoffmann, E. Ramirez, J. D. Taupin, Coherent isotope history of Andean ice cores over the last century, Geophys. Res. Lett. 30(2003)1179-1182.

[5] J. P. Steffensen, K. K. Andersen, M. Bigler, H. B. Clausen, D. Dahl-Jensen, E. Al, High-resolution Greenland ice core data show abrupt climate change happens in few years, Science. 321(2008)680-684.

[6] C. Sturm, Q. Zhang, D. Noone, An introduction to stable water isotopes in climate models: benefits of forward proxy modelling for paleoclimatology, CLIM. PAST. 6(2010) 115-129.

[7] D. Noone, C. Sturm, Comprehensive dynamical models of global and regional water isotope distributions, Springer. 2010: 195-219.

[8] D. Hofstetter, J. D. Francesco, L. Hvozdara, H. P. Herzig, M. Beck, CO 2 isotope sensor using a broadband infrared source, a spectrally narrow 4.4 μm quantum cascade detector, and a fourier spectrometer, Appl. Phys. B. 103(2011)967-970.

[9] L. F. Han, M. Gröning, P. Aggarwal, Reliable determination of oxygen and hydrogen isotope ratios in atmospheric water vapour adsorbed on 3A molecular sieve, Rapid Commun. Mass Spectrom. 20(2006)3612-3618.

[10] J. A. Karhu, Catalytic reduction of water to hydrogen for isotopic analysis using zinc containing traces of sodium, Anal. Chem. 69 (1997)4728-4730.

[11] J. Bigeleisen, M. L. Perlman, and H. Ct Prosser, Conversion of hydrogenic materials to hydrogen for isotopic analysis, Anal. Chem. 24 (1952)1356-1357.

[12] E.R.T. Kerstel, G. Gagliardi, L. Gianfrani, H.A.J. Meijer, R. van Trigt, R. Ramaker, Determination of the 2H/1H, 17O/16O, and 18O/16O isotope ratios in water by means of tunable diode laser spectroscopy at 1.39 μm, Spectrochimica Acta Part A 58 (2002) 2389–2396.

[13] E. R. T. Kerstel, R. Van Trigt, J. Reuss, Simultaneous determination of the 2H/1H, 17O/16O, and 18O/16O isotope abundance ratios in water by means of laser spectrometry, Anal. chem. 71(1999)5297-5303.

[14] E. R. T. Kerstel, R.Q. Iannone, M. Chenevier, S. Kassi, H.-J. Jost, D. Romanini, A water isotope (2H, 17O, and 18O) spectrometer based on optical feedback cavity-enhanced absorption for in situ airborne applications, Appl. Phys. B 85(2006)397–406.

[15] J. Landsberg, D. Romanini, E. Kerstel, Very high finesse optical-feedback cavity-enhanced absorption spectrometer for low concentration water vapor isotope analyses, Opt. Lett. 39(2014)1795-1798.

[16] A. Castrillo, H. Dinesan, G. Casa, G. Galzerano, P. Laporta and L. Gianfrani, Amount-ratio determinations of water isotopologues by dual-laser absorption spectrometry, PHYSICAL REVIEW A 86(2012)052515.

[17] L. Gianfrani, G. Gagliardi, M. van Burgel, and E. R. Th. Kerstel, Isotope analysis of water by means of nearinfrared dual-wavelength diode laser spectroscopy, Opt. Express 11(2003) 1566-1576.

[18] C. Dyroff, D. FŘtterer, A. Zahn. Compact diode-laser spectrometer ISOWAT for highly sensitive airborne measurements of water-isotope ratios, Appl. Phys. B. 98(2010)537-548.

[19] T. Wu, W. Chen, E. Kerstel, Kalman filtering real-time measurements of H2O isotopologue ratios by laser absorption spectroscopy at 2.73 μm, Opt. Lett. 35(2010)634-636.

[20] T. Wu, W. Chen, E. Fertein, Measurement of the D/H, 18O/16O, and 17O/16O isotope ratios in water by laser absorption spectroscopy at 2.73 μm, Sensors. 14(2014)9027-9045.

[21] X. Cui, W. Chen, M. W. Sigrist, E. Fertein, P. Flament, K. De Bondt, N. Mattielli, Analysis of the Stable Isotope Ratios ($^{18}O/^{16}O$, $^{17}O/^{16}O$, and D/H) in Glacier Water by Laser Spectrometry. Anal. Chem. 92(2020)4512–4517.

[22] J. B. Mcmanus, D. D. Nelson, M. S. Zahniser, Design and performance of a dual-laser instrument for multiple isotopologues of carbon dioxide and water, Opt. Express. 23(2015)6569-86.

[23] X. Lee, S. Sargent, R. Smith, B. Tanner, In Situ Measurement of the Water Vapor 18O/16O Isotope Ratio for Atmospheric and Ecological Applications, J. Atmos. Ocean. Tech. 22(2005)555-565.

[24] X. Wen, X. Sun, S. Zhang, G. Yu, S. D. Sargent, X. Lee, Continuous measurement of water vapor D/H and 18O/16O isotope ratios in the atmosphere, J. Hydrol. 349(2008)489-500.

[25] D. S. Sayres, E. J. Moyer, T. F. Hansco, A new cavity based absorption instrument for detection of water isotopologues in the upper troposphere and lower stratosphere, Rev. Sci. Instrum. 80(2009)044102.

[26] W. E. Wang, A. Michel, L. Wang, A quantum cascade laser-based water vapor isotope analyzer for environmental monitoring, Rev. Sci. Instru. 85(2014)235-787.

[27] https://www.picarro.com.

[28] http://www.lgrinc.com.

[29] E. Garmire, T. McMahon, M. Bass, Propagation of infrared light in flexible hollow waveguides, Appl. Opt. 15(1976)145–150.

[30] P. Jaworski, K. Krzempek, P. Kozioł, D. Wu, F. Yu, P. Bojęs, G. Dudzik, M. Liao, J. Knight, K. Abramski, Sub parts-per-billion detection of ethane in a 30-meters long mid-IR Antiresonant Hollow-Core Fiber, Opt. Laser Technol. 147(2022)107638.

[31] J. Westberg, J. Wang, O. Axner. Fast and non-approximate methodology for calculation of wavelength-modulated Voigt lineshape functions suitable for real-time curve fitting, J. Quant. Spectrosc. Radiat. Transf. 113(2012)2049-2057.

[32] H. A. J. Meijer, and W. J. Li, The use of electrolysis for accurate $\delta^{17}O$ and $\delta^{18}O$ isotope measurements in water, Isot. Environ. Healt. S, 34(1998) 349-369.

[33] D. W. Allan. Statistics of atomic frequency standards, P. IEEE, 54(1966)221-230.

[34] Gregory J. Fetzer, Anthony S. Pittner, William L. Ryder, and Dorothy A. Brown,Tunable diode laser absorption spectroscopy in coiled hollow optical waveguides, Appl. Opt. 41(2002)3613-3621.

[35] H. Riris, C. B. Carlisle, R. E. Warren. Kalman filtering of tunable diode laser spectrometer absorbance measurements, Appl. Opt. 33(1994)5506-5508.

[36] D. P. Leleux, R. Claps, W. Chen, Applications of Kalman filtering to real-time trace gas concentration measurements, Appl. Phys. B. 4(2002)85-93.

Credit Author Statement

Yang Liu: Investigation, Writing - original draft. **Tao Wu:** Conceptualization, Funding acquisition, Writing - Review & Editing. **Qiang Wu:** Writing - Review & Editing. **Weidong Chen:** Writing - Review & Editing. **Chenwen Ye:** Investigation. **Mengyu Wang:** Investigation. **Xingdao He:** Conceptualization.